JOURNAL OF AIRCRAFT
Vol. 40, No. 3, May–June 2003

Flight Testing with the Flutterometer

Rick Lind*
University of Florida, Gainesville, Florida 32611-6250

The flutterometer is an on-line tool that indicates a measure of distance to flutter in terms of a flight condition during a flight test. The measure of distance is computed as a robust flutter margin by applying μ-method analysis to consider the worst-case effects of modeling uncertainty. The approach is to update the robust flutter margin at a series of test points by analyzing flight data. The flutterometer was used during an envelope expansion of the Aerostructures Test Wing. This paper describes the results of that flight test. Algorithm and implementation details that are critical to the successful application of the tool are discussed. Also, flight data and analysis are presented to demonstrate the flutterometer operation. The flight test demonstrated that the flutterometer is able to predict a conservative estimate of the flutter speed.

Introduction

FLIGHT flutter testing is the process of envelope expansion to determine a range of flight conditions within which an aircraft is safe from aeroelastic instabilities such as flutter. This testing, which must be done for new and modified aircraft, incurs dramatic time and costs because of the danger associated with encountering unpredicted instabilities. The common approach for envelope expansion is to take the aircraft to a stabilized test point and measure vibration data. Data from the test points are analyzed to predict the speed at which flutter might be encountered. The envelope is expanded by increasing the airspeed at successive test points until the data analysis indicates that airspeed is nearing the flutter speed.

Several methods are traditionally used for the data analysis and prediction of the flutter speed. The most common method is to analyze damping levels that vary with flight condition and extrapolate the resulting trends.[1] Another common method is to use the concept of a flutter margin in conjunction with a formulation to predict the onset of flutter.[2] Each of these methods has proven useful for flight-test programs; however, their predictions are never accepted with complete confidence. Certainly damping will decrease to zero as the aircraft approaches flutter, but the nonlinear variation of damping with airspeed can make accurate extrapolation difficult. Similarly, the flutter margin is technically correct for low-order flutter, but it will predict the correct speed only if the flutter mechanism is actually low-order and accurate dampings are computed for the necessary modes. Thus, these methods are valuable but must be applied with caution.

The flutterometer is a tool designed to predict the onset of flutter with more confidence than traditional approaches.[3] In particular, this tool is able to compute a worst-case estimate of the flutter speed that is conservative with respect to the true flutter speed. In this way the flutterometer can be used to augment the traditional tools so that a set of flutter speeds are predicted. The increased reliability of the flutterometer at low speeds allows the testing to proceed more rapidly and safely.

The validity of the flutterometer must be extensively tested to ensure its usefulness to the flight-test community. A series of tests that used wind tunnels and flight systems to demonstrate the properties of the flutterometer were conducted. One particularly interesting test involved the Aerostructures Test Wing (ATW). The ATW was a wing structure that was attached to the undercarriage of an F-15 aircraft. This setup allowed the system to be tested at flight conditions that were safe for the F-15 but resulted in aeroelastic instabilities for the ATW. An envelope expansion of the ATW was conducted until the onset of flutter. Flight data from that expansion were analyzed by traditional methods and the flutterometer to evaluate the predictive capabilities of each approach.

This paper details the results of the flight-test program for the ATW. In particular, the flutterometer is evaluated and discussed. One aspect of the discussion considers the preflight development that involved coordinating information and requirements for modeling, ground vibration testing, flight procedures, computational assets, and control room issues. Another aspect of the discussion describes the operation and performance of the flutterometer.

Flutterometer

The flutterometer is a tool that predicts flutter margins during a flight test. This tool is inherently different from traditional approaches that attempt to predict the onset of flutter. These differences include the type of information used in the computation, the type of analysis performed by the tool, and the type of prediction that results.

Fundamentally, the flutterometer is a model-based tool. This description is intended to note that the flutter margin is computed by analyzing the stability properties of an analytical model. In this respect the flutterometer is similar to standard computational approaches; however, the flutterometer differs in that this tool also uses flight data to formulate characteristics of the model. This tool actually uses both analytical models and flight data. Thus, the type of information used by the flutterometer is different from other approaches.

The basis for the flutterometer is μ-method analysis.[4] The μ-method analysis computes a stability measure that is robust with respect to an uncertainty description.[5] The resulting robust flutter speed is worst case with respect to that uncertainty. The flutterometer operates by computing an uncertainty that is representative of modeling errors as noted by analyzing flight data. In this way the flutterometer predicts a realistic flutter speed that is more beneficial than theoretical predictions because the robust speed directly accounts for flight data. Thus, the type of analysis performed by the flutterometer is significantly different from standard aeroelastic analysis.

The flutter margin that is computed by the flutterometer is actually the robust flutter margin for the analytical model with respect to the uncertainty. This margin is mathematically valid based on the aeroelastic dynamics as indicated by the model. In this way the tool is analytically predictive as opposed to the ad hoc predictions that result from extrapolating damping trends or assumptions of general binary flutter. In this way the type of prediction is considerably different from traditional approaches.

The theoretical aspects of the flutterometer have been previously presented[3] and so are not reproduced here. Instead, this paper will

Received 4 October 2001; revision received 9 May 2002; accepted for publication 10 May 2002.

*Assistant Professor, Department of Mechanical and Aerospace Engineering, 321 Aerospace Building; rick@aero.ufl.edu. Member AIAA.

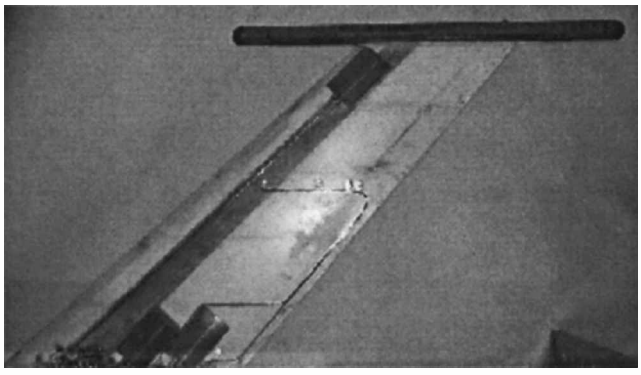

Fig. 1 Aerostructures test wing.

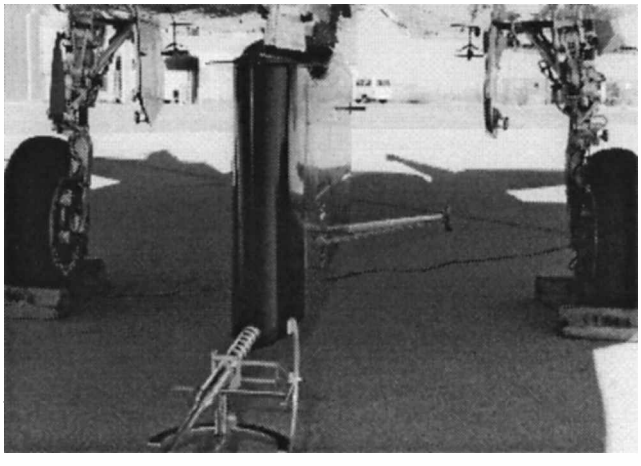

Fig. 2 Aerostructures test wing mounted to F-15.

concentrate on a general evaluation of using the tool for a flight-test program.

Aerostructures Test Wing

The ATW was developed at NASA Dryden Flight Research Center. The ATW was essentially a wing and boom assembly as shown in Fig. 1. This assembly was flown by using an F-15 aircraft and associated flight-test fixture. The ATW is mounted horizontally to the fixture, and the resulting system attaches to the undercarriage of the F-15 fuselage as shown in Fig. 2. Previous testing indicated that the airflow is relatively smooth around the system so that the F-15 fuselage and wings are assumed to have minimal interference with the ATW.

The wing was formulated based on a NACA-65A004 airfoil shape. The wing had a span of 18.0 in. with root chord length of 13.2 in. and tip chord length of 8.7 in. The boom was a 1-in.-diam hollow tube of length 21.5 in. The total weight of the ATW was 2.66 lb.

The ATW was meant to be a realistic testbed that represents complexity of an aircraft component; however, the construction of the testbed was limited by safety concerns. These potentially conflicting issues were addressed by designing the ATW with a rib and spar construction that uses lightweight materials with no metal. Specifically, the skin and spar were constructed from fiberglass cloth, the boom was constructed from carbon fiber composite, the wing core was constructed from rigid foam, and components were attached by epoxy. Also, powdered tungsten was included in the endcaps of the boom for mass balancing. The system was designed to flutter at a subsonic condition within the flight envelope of the host F-15.

A measurement and excitation system was incorporated into the wing. The measurement system consisted of 18 strain gauges placed throughout the airfoil structure and 3 accelerometers placed at fore, aft, and midlocations in the boom. The excitation system was 6 patches of piezoelectric material, 3 patches mounted on the upper surface that are out of phase with 3 patches on the lower surface, that acted as a single distributed actuator. Sinusoidal sweeps of energy from 5 to 35 Hz were commanded to these patches.

Table 1 Measured structural modes of the ATW

Mode	Frequency, Hz
1st bending	14.05
1st torsion	22.38
2nd bending	78.54

Ground vibration tests were conducted to determine the structural dynamics of the wing. The main modes of the system and their natural frequencies are presented in Table 1. Tests were conducted for the wing on a test stand and also attached to the flight-test fixture to ensure that these modal properties were not affected for the flight testing.

Flutterometer Development

Model

The flutterometer is a state-space model-based analysis tool, and, consequently, the formulation of a model is of paramount importance. A standard method is to first generate a finite element model that represents the structure, compute unsteady aerodynamics using approaches such as doublet lattice theory, and then formulate a state-space model using rational functional approximations. This standard method was initially adopted for the ATW; however, there were several unexplained sensitivity and conditioning issues. For instance, minor alterations in mass of the structure resulted in extremely large variations in predicted flutter speed. Also, the model was unable to simultaneously match both the natural frequencies and mode shapes as measured by the ground vibration test. Consequently, the finite element model was not used for flutterometer development.

An approach was used to generate a model of the ATW that combined elements from a finite element model with data from the ground vibration testing. A finite element model was initially used to generate a set of mass values at locations throughout the structure. Correspondingly, the test data indicated the frequencies and responses at these locations for modes of the structure. An equivalent model was then formulated with natural frequencies and modes shapes that were determined by the data, mass values that were purely analytical, and stiffness values that resulted from relating the analytical mass and experimental natural frequencies. This equivalent model was thus representative of both analytical and experimental results. This model was formulated using the ZAERO package.

The first use of the equivalent model was to generate a state-space representation of the structural dynamics of the ATW. This representation resulted from generating a reduced-order model of mass and stiffness values that were associated with the modes of Table 1. The equivalent model did not use any structural damping, and so a modal damping matrix was determined directly by the test data. This determination was a straightforward procedure based on system identification results.

Also, the structural model was augmented to include the excitation and sensing elements. An input matrix was generated that noted the effects of the excitation system on the structural dynamics. Similarly, an output matrix was generated that noted the responses of the accelerometers throughout the structure. Each of these matrices was identified directly from the data of the ground vibration test. These matrices were generated with a relatively high amount of confidence because the excitation system is actually a structural excitation system that affects strains and stresses rather than an aerodynamic excitation system such as control surfaces. Thus, the input and output matrices could be completely determined entirely from ground vibration testing.

The quality of the structural model is evidenced by comparing transfer functions from the model and the test data. These transfer functions relate the input command to the excitation system and the output responses from the accelerometers in the boom. Figure 3 compares transfer functions from model and data for the accelerometer at the trailing edge of the boom. This comparison

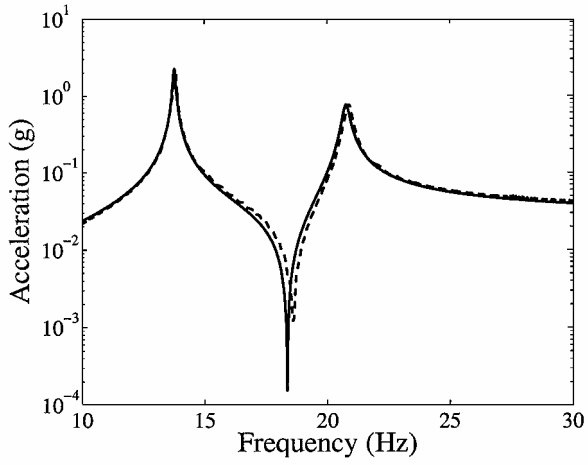

Fig. 3 Transfer functions from excitation system to accelerometer at boom trailing edge for data (- - - -) and model (——).

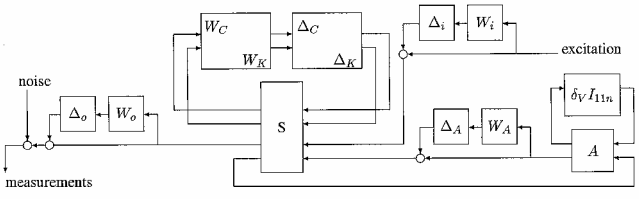

Fig. 4 Uncertain model of the aerostructures test wing.

demonstrates that the structural model was able to accurately reproduce the dynamics as observed in the data.

The second use of the equivalent model was to generate a state-space representation of the unsteady aerodynamic forces. The equivalent model was used directly by standard computational tools to compute the aerodynamic forces and flutter speeds. These forces were computed as a set of complex matrices for a set of distinct reduced frequencies. A state-space representation of the forces was then generated by approximating the set of matrices as a rational function.[6]

The analysis of the equivalent model resulted in a state-space model of the structural dynamics and a state-space model of the aerodynamics. These models needed to be altered to fit into the μ-method framework and also combined to generate an aeroelastic model. This procedure is quite straightforward as documented in the literature.[7] The model is put into the μ-method framework by parameterizing the elements around flight condition and adding uncertainties. Then, the generation of a single aeroelastic model is accomplished by relating the structural and aerodynamic models by feedback.

The parameterization around flight condition is accomplished by noting the dependence of the aerodynamics on airspeed. The concept is to replace the airspeed parameter with a summation of a nominal airspeed and a perturbation. The explicit dependence of the dynamics on this perturbation is then replaced by an equivalent dependence through feedback for the nominal value and the perturbation.

The introduction of uncertainties actually made use of both the structural and aerodynamic representations. One type of uncertainty that was introduced is parametric uncertainty. Uncertainty operators are directly associated with the stiffness and damping matrices of the structural dynamics. Another type of uncertainty that was introduced is dynamic uncertainty. This type of uncertainty is associated with the magnitude and phase of the aerodynamic forces. Also, dynamic uncertainty was associated with the excitation and sensing signals to account for the effects of unmodeled dynamics and mode shape errors.

The aeroelastic model in the μ-method framework is shown in Fig. 4. The elements of this model are easily seen. In particular, the structural dynamics are noted as S, and the aerodynamics are noted as A. The perturbation to airspeed δ_V appears in association with the aerodynamics because that block contains all of the velocity dependency. Also, the parametric and dynamic uncertainties are shown in relation to the elements with which they are associated. The elements Δ_K and Δ_C are the parametric uncertainties associated with stiffness and damping, Δ_A is the dynamic uncertainty associated with the aerodynamic forces, and Δ_i and Δ_o are the dynamic uncertainties associated with input and output signals. Each of these operators is weighted to reflect a desired level of uncertainty. For example, the operator Δ_K is restricted to be norm bounded by unity so that the weighting W_K scales the loop and allows consideration of errors that are not of unity size. The actual values of the weightings will be determined by analysis of flight data.

Implementation

The flutterometer was implemented for ATW testing as a MATLAB® process. In actuality, there were several processes that operated in conjunction. The flutterometer, as referred to in this paper, implies the process that computes on-line robust flutter margins. The other processes deal with data transfer. Essentially, the processes operated independently; however, the proper operation of the flutterometer depended on an implementation that allows these processes to communicate efficiently.

The overall flowchart for the flutterometer implementation traces the data from aircraft telemetry to the generation of a robust flutter margin. There are many steps in this flowchart; however, the implementation can effectively be viewed as three steps.

The first step in the flutterometer implementation was to gather data from the aircraft telemetry stream. This step was done using a framework for data networking called the ring buffered network bus (RBNB).[8] The concept used for ATW testing had an RBNB process transferring data from the telemetry stream to a memory cache. The data in the cache were converted from generic telemetry units, such as counts, into engineering units, such as acceleration in g, for use with analysis processes. Also, the cache contained all signals from the entire flight. In this way the cache acted like an on-line data server from which any data that were gathered during the flight could be immediately accessed.

The second step in the implementation was to provide an interface that linked the data server with MATLAB. This software was written as a MATLAB process that ran continuously and monitored the data cache. The concept behind this process was to poll the data until a condition was satisfied that indicated data should be transferred. This trigger condition for the ATW testing was a signal that was nonzero only while the excitation system is active. The interface process transferred a block of data, corresponding to a continuous stream of data with a nonzero excitation signal, between the data cache and the local analysis computer. Also, the interface system converted the data from an RBNB format into a MATLAB structure. The data were then saved as a file with a unique identifier that corresponded to the time at which the data were generated.

The third step was to analyze the data and compute a robust flutter margin. This step was the flutterometer process and was entirely a MATLAB function. The process began by loading a user-specified data file. The flight conditions associated with the data file were noted, and a corresponding model was loaded. The process then continued by generating uncertainty levels and performing a μ analysis to compute an on-line flutter margin.

The interaction between the user and the implementation was only in the third step. The first and second steps were initialized with information about the telemetry stream and the trigger condition and then run autonomously. The third step was not as deterministic and thus was required to be monitored. Some of the parameters that were allowed to be changed during a flight were the frequencies for model validation and μ analysis, the updating scheme for the uncertainty levels, the flight condition units of the flutter margin, the sensors to be considered for analysis, and various display options. The flutterometer employed an interface that allows these options to be changed by simple graphical entries.

Control Room Procedures

The control room procedures for flight flutter testing are a set of well-established methods that maximize safety and efficiency of the testing. The introduction of a new tool into this environment required

these procedures to be properly augmented. Clearly the flutterometer is a departure from traditional analysis methods, and so the control room must properly account for this additional information.

The envelope expansion of the ATW occurred using standard procedures. Namely, the system was flown to a stabilized test point and remained on condition while response data were measured. The control room evaluated these data and determined whether the aircraft could increase speed until arriving at the next test point.

The main tool that was used to determine the envelope expansion was the analysis of damping. The response data that described the modal dynamics of the first bending and first torsion modes were carefully monitored to note any trends that indicated destabilizing properties.

The flutterometer was also used for information about unstable flight conditions; however, it was not the main tool. The reason for this was that the flutterometer should be somewhat conservative. This tool should predict a worst-case indication of flutter margin, and so it should predict a loss of stability for flight conditions that are only close to instability. One valuable piece of information from the ATW testing is an indication of the actual level of conservatism in the flutterometer. Therefore, the wing needed to be flown past the flutterometer margin until the damping trends clearly indicated the imminent onset of flutter. At this point the true flutter speed was known, and an evaluation of the predictive properties of damping and the flutterometer could be made.

Flight Test

Flight Operation

Flight tests of the ATW were performed on five different dates throughout March and April 2001 at NASA Dryden Flight Research Center. These flights performed an envelope expansion that used a series of test points with increasing dynamic pressure. The initial test points were chosen as some of the lowest dynamic pressures at which the host F-15 aircraft can effectively operate. There were a total of 21 test points used during these flights. The flight conditions at the points ranged from Mach 0.50 to 0.85 with altitudes between 10,000 and 20,000 ft.

The flight test for envelope expansion was to follow standard procedures for test point operation. Specifically, the aircraft arrived on condition and then flew straight and level for 30 s to gather information about turbulence levels. After the stabilized run the excitation system on the ATW was activated, and response data were measured. These response data were telemetered to the control room and analyzed by damping and flutterometer algorithms. Also, wind-up turns and push-over/push-up maneuvers were performed to gather information about loads on the ATW.

Test Point Analysis

Consider the analysis at the test point with a speed of Mach 0.60 and altitude of 20,000 ft during the flight. Response data were generated by commanding a 60-s sine sweep from 5 to 35 Hz to the excitation system of the ATW. The measured response of the leading-edge boom accelerometer is shown in Fig. 5.

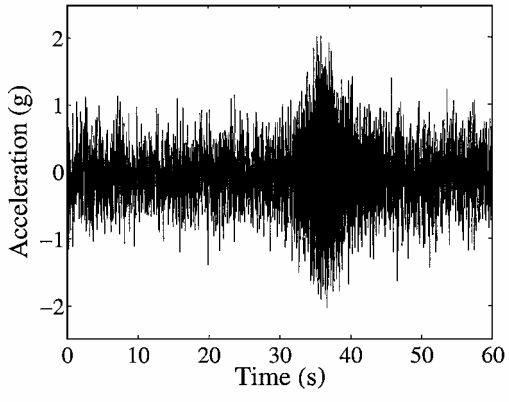

Fig. 5 Response of the leading-edge boom accelerometer to a sine sweep excitation.

The data in Fig. 5 indicate that a high level of noise is present in the measurements. This level of noise was not observed in the ground or taxi tests; rather, it appears to be the inherent level observed in flight. The data from other test points are not shown here, but they indicated this same level of noise. The cause of the noise is not known, but suspected causes include slight turbulence on the system and also vibrations resulting from engine operation.

Also, the only mode that can be clearly observed in the time domain is the torsion mode. Simulations predicted that the bending mode would be observable above the noise level, but this was proven incorrect. The noise is relatively broadband, but simple filtering and averaging techniques were employed such that bending can indeed be clearly seen in the frequency-domain transfer functions despite the limited time-domain observability.

One analysis of the data is to estimate the damping properties. A standard approach that uses system identification algorithms is used for this analysis. The analysis determines that the first bending mode, at this condition, has a natural frequency of 16.5 Hz and -0.112 for the structural damping. Similarly, the first torsion mode at this condition is estimated to have a natural frequency of 22.6 Hz and -0.106 for the structural damping.

The other analysis of the data is to compute a robust flutter margin. This analysis is accomplished by the flutterometer. The data are used by the flutterometer to note differences between the data and the analytical model. These differences could be used for further model updating beyond the simple removal of bias that was already performed; however, the differences are only considered to be errors in the model for purposes of this paper.

The uncertainty levels associated with the analytical model are initially small but are allowed to increase at each test point. In particular, the uncertainty is increased until the measured data do not invalidate the analytical model. The basic concept of this validation is to check that the measured data lie within upper and lower bounds on the range of transfer functions for the uncertain model. Figure 6 demonstrates this concept for the test point analysis.

The model in Fig. 6 has enough uncertainty so the data essentially lie within the upper and lower bounds. These uncertainty levels correspond to 4% parametric error in structural stiffness, 73% parametric error in structural damping, 2% dynamic error in the aerodynamic forces, 70% dynamic error in the sensor measurements, and 18% dynamic error in the excitation energy. These values might seem quite large; however, the flutter speed is most strongly influenced by the small uncertainties in structural stiffness and aerodynamic forces. The flutterometer determined that these levels were required so the data did not invalidate the model.

A μ-method analysis is computed on the uncertain model. The resulting robust flutter speed is 405 KEAS. This speed is significantly lower than the 445 KEAS that represents the nominal flutter speed of the Mach 0.60 model. Thus, the flutterometer has detected errors in the model and computed a worst-case flutter speed that accounts

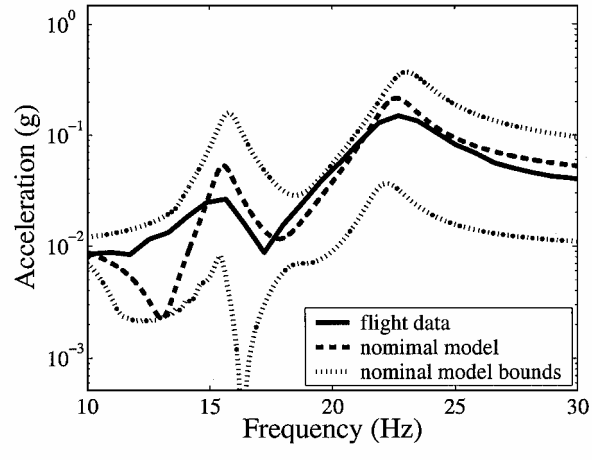

Fig. 6 Transfer functions from the excitation to response of the leading-edge boom accelerometer: - - - -, flight data; ——, analytical model; and · · · ·, bounds on range of analytical model.

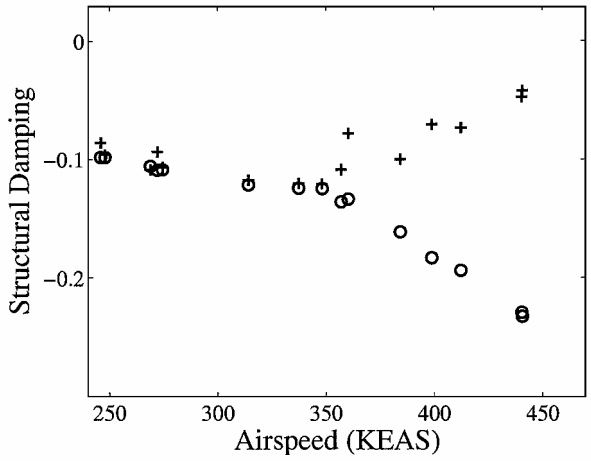

Fig. 7 Measured modal dampings for bending mode (+) and torsion mode (○).

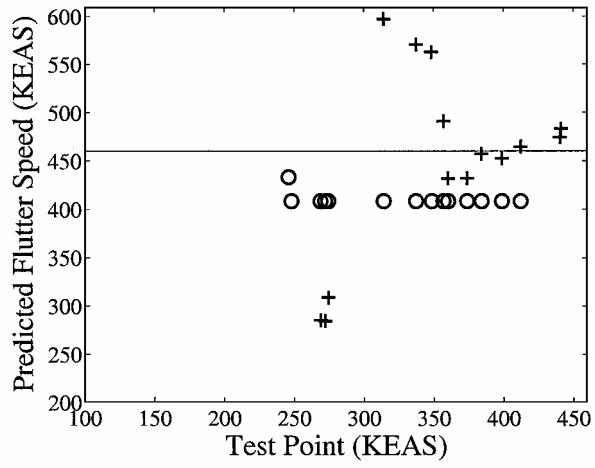

Fig. 8 Predicted flutter speeds during envelope expansion from damping trends (+) and flutterometer (○).

for these errors. This is directly in contrast to the damping analysis that demonstrates the stability of the ATW but is unable to indicate any predictive capability after a single test point.

Envelope Expansion

The flight test of the ATW was an envelope expansion that included 21 test points. The speed and dynamic pressure were increased between each test point. The final test point at which data were taken was near Mach 0.825 and 10,000 ft. Flutter was encountered during the acceleration from this test point to the next planned test point. The data indicate that flutter was encountered at approximately Mach 0.83 and 10,000 ft.

The data from each of the test points are used to estimate levels of structural damping. These levels are computed and plotted as a function of airspeed in Fig. 7. This plot only shows results from data sets that had clearly observable modes. The bending mode was particularly difficult to observe at several test points, and so damping values were not estimated at these conditions.

The onset of flutter can be clearly seen in the damping values. The torsion mode is becoming more damped, whereas the bending mode is becoming less damped as the airspeed increases. The conventional flutter mechanism for such a system is usually assumed to result in the torsion mode becoming less stable; however, the ATW results can still be considered a classical flutter mechanism in the sense that one mode is becoming more stable while the other becomes less stable.

The complete set of damping values indicates the onset of flutter; however, these values also indicate the difficulty in predicting the onset of flutter. Consider that the structural damping for the bending mode does not indicate an adverse trend until a speed of at least 375 KEAS. Thus, damping is shown to be a poor predictor of flutter for the ATW until the system is operated at speeds perilously close to the flutter boundary.

Predictions of the flutter speed were computed at every test point. Several predictions methods were utilized; however, this paper will only consider the predictions from the flutterometer and damping extrapolation. The predicted speeds are given in Fig. 8. Clearly the flutterometer is able to predict a conservative estimate.

An interesting feature to note in Fig. 8 is that the predicted speed from the flutterometer does not change after the initial test point. This feature results from the uncertainty description remaining basically unchanged throughout the flight test. Essentially, the initial test point indicated an amount of modeling error that was sufficient to account for data acquired at later test points. This indicates that the flutterometer identified the modeling errors immediately and accounted for them. In this way a reasonable flutter speed was computed by the flutterometer much earlier than that predicted by the damping trends.

Another feature to note in Fig. 8 is that the conservatism in the flutterometer prediction does not decrease as the envelope is expanded.

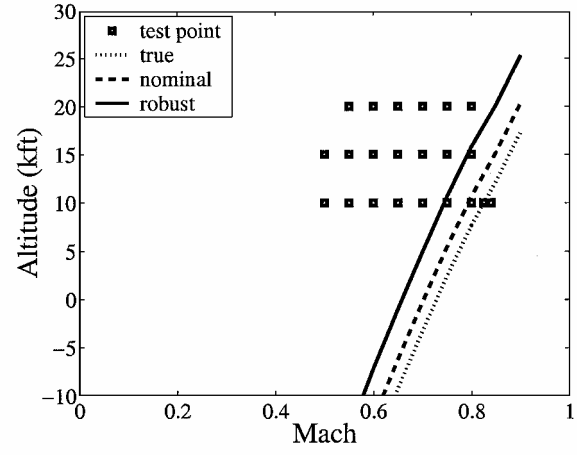

Fig. 9 Flutter speeds of the ATW.

This feature remains even as flight data are analyzed from points beyond the robust flutter speed. Essentially, the implementation of the flutterometer for the ATW allowed the uncertainty level to only increase, and never decrease, during the flight. This implementation is the most conservative approach among several possibilities, but it also is considered the safest. The ATW used this conservative approach in part to test the level of conservatism.

Robust Flutter Speeds

The robust flutter speeds are actually computed as a function of Mach number. These speeds are presented in Fig. 9 along with the nominal flutter speeds of the analytical model.

The robust flutter speeds that are computed by the flutterometer are less than the nominal flutter speeds. This result is expected when considering the data shown in Fig. 6. Specifically, the initial model cannot reproduce the flight data so that uncertainty must be associated to account for the errors. Such errors are noted at all test points. The robust speeds account for these errors and represent worst-case results.

The flutterometer indicates the potential for flutter occurs at airspeeds near 405 KEAS for a Mach 0.60 and 405 KEAS for Mach 0.80 flight conditions. In actuality, the envelope expansion demonstrated that flutter occurs at Mach 0.83 and 460 KEAS. Therefore, the flutterometer has clearly predicted a conservative flutter speed.

The conservatism in the flutterometer prediction is actually an expected, and desired, result. The flutterometer is mathematically conservative, but the excessive conservatism in Fig. 9 is largely caused by the analytical model. This model has errors such that the analytical flutter speed is lower than the true flutter speed. The flutterometer noted these errors and computed a worst-case flutter speed. This worst-case speed is always less than the analytical flutter

speed so that the flutterometer is even more conservative than the analytical model. Thus, the flutterometer performed as expected, but the results are somewhat limited because of the inherent conservatism in the model.

The analysis of Fig. 9 indicates the conservatism in the flutterometer predictions; however, this analysis also indicates a shortcoming in the flutterometer. Specifically, a formal approach for model updating should be integrated with the μ-method analysis. A robust flutter analysis of the ATW is essentially guaranteed to be conservative because the nominal model is already conservative. A valuable test that is currently under investigation is to generate an accurate model of the ATW and demonstrate the flutterometer still computes conservative flutter speeds with this nonconservative model.

Conclusions

This paper describes issues associated with the flutterometer during a flight test of the Aerostructures Test Wing. These issues include model development, control room implementation, and data analysis. It is shown the flutterometer can be easily implemented in a control room and operated using standard flight-test procedures. Also, the flight test indicates the predictive nature of the flutterometer. In particular, the generation of uncertainty levels is clearly seen by the analysis of flight data. The corresponding robust flutter speeds are computed and indicate the worst-case stability margins with respect to the uncertainty. This flight test indicates that the flutterometer is a tool with reasonable computational cost that provides significant beneficial information.

References

[1]Kehoe, M. W., "A Historical Overview of Flight Flutter Testing," NASA-TM-4720, Oct. 1995.

[2]Zimmerman, N. H., and Weissenburger, J. T., "Prediction of Flutter Onset Speed Based on Flight Testing at Subcritical Speeds," *Journal of Aircraft*, Vol. 1, No. 4, 1964, pp. 190–202.

[3]Lind, R., and Brenner, M., "The Flutterometer: An On-Line Tool to Predict Robust Flutter Margins," *Journal of Aircraft*, Vol. 37, No. 6, 2000, pp. 1105–1112.

[4]Lind, R., and Brenner, M., *Robust Aeroservoelastic Stability Analysis*, Springer-Verlag, London, 1999, pp. 111–116.

[5]Packard, A., and Doyle, J., "The Complex Structured Singular Value," *Automatica*, Vol. 29, No. 1, 1993, pp. 71–109.

[6]Karpel, M., "Design for Active Flutter Suppression and Gust Load Alleviation Using State-Space Aeroelastic Modeling," *Journal of Aircraft*, Vol. 19, No. 3, 1982, pp. 221–227.

[7]Lind, R., "Match-Point Solutions for Robust Flutter Analysis," *Journal of Aircraft*, Vol. 39, No. 1, 2002, pp. 91–99.

[8]Freudinger, L. C., Miller, M. J., and Kiefer, K., "A Distributed Computing Environment for Signal Processing and Systems Health Monitoring," *Proceedings of the AIAA/IEEE/SAE Digital Avionics Systems Conference*, Inst. of Electrical and Electronics Engineers, Piscataway, NJ, 1998, pp. C35/1–C35/8.